Am J Physiol Renal Physiol 294: F414–F422, 2008.
First published December 12, 2007; doi:10.1152/ajprenal.00174.2007.

Dipeptidyl peptidase IV inhibition downregulates Na^+-H^+ exchanger NHE3 in rat renal proximal tubule

Adriana Castello Costa Girardi, Lívia Emy Fukuda, Luciana Venturini Rossoni, Gerhard Malnic, and Nancy Amaral Rebouças

Department of Physiology and Biophysics, Institute of Biomedical Sciences, University of São Paulo, São Paulo, Brazil

Submitted 12 April 2007; accepted in final form 6 December 2007

Girardi AC, Fukuda LE, Rossoni LV, Malnic G, Rebouças NA. Dipeptidyl peptidase IV inhibition downregulates Na^+-H^+ exchanger NHE3 in rat renal proximal tubule. *Am J Physiol Renal Physiol* 294: F414–F422, 2008. First published December 12, 2007; doi:10.1152/ajprenal.00174.2007.—In the microvillar microdomain of the kidney brush border, sodium hydrogen exchanger type 3 (NHE3) exists in physical complexes with the serine protease dipeptidyl peptidase IV (DPPIV). The purpose of this study was to explore the functional relationship between NHE3 and DPPIV in the intact proximal tubule in vivo. To this end, male Wistar rats were treated with an injection of the reversible DPPIV inhibitor Lys[$Z(NO_2)$]-pyrrolidide (I40; 60 $mg \cdot kg^{-1} \cdot day^{-1}$ ip) for 7 days. Rats injected with equal amounts of the noninhibitory compound Lys[$Z(NO_2)$]-OH served as controls. Na^+-H^+ exchange activity in isolated microvillar membrane vesicles was 45 ± 5% decreased in rats treated with I40. Membrane fractionation studies using isopycnic centrifugation revealed that I40 provoked redistribution of NHE3 along with a small fraction of DPPIV from the apical enriched microvillar membranes to the intermicrovillar microdomain of the brush border. I40 significantly increased urine output (67 ± 9%; $P < 0.01$), fractional sodium excretion (63 ± 7%; $P < 0.01$), as well as lithium clearance (81 ± 9%; $P < 0.01$), an index of end-proximal tubule delivery. Although not significant, a tendency toward decreased blood pressure and plasma pH/HCO_3^- was noted in I40-treated rats. These findings indicate that inhibition of DPPIV catalytic activity is associated with inhibition of NHE3-mediated $NaHCO_3$ reabsorption in rat renal proximal tubule. Inhibition of apical Na^+-H^+ exchange is due to reduced abundance of NHE3 protein in the microvillar microdomain of the kidney brush border. Moreover, this study demonstrates a physiologically significant interaction between NHE3 and DPPIV in the intact proximal tubule in vivo.

sodium transport; proton secretion; fluid reabsorption; serine protease

IN THE KIDNEY, THE ACTIVITY of the Na^+-H^+ exchanger isoform NHE3, located at the apical membrane of the proximal tubule, plays a key role in mediating the active, transcellular reabsorption of $NaHCO_3$ and NaCl (1, 4, 5, 26, 38, 44–46). Tight regulation of NHE3 activity is therefore critical for the maintenance of volume and acid-base homeostasis.

Numerous physiological and humoral factors were reported to affect NHE3 activity, and although many of them share the same signaling pathways, their final response may differ greatly (7, 32). The recent identification of regulatory proteins that interact with NHE3 has unraveled some aspects of the molecular mechanisms underlying the transporter regulation (8, 32). By means of coprecipitation experiments, Girardi and colleagues (11) previously demonstrated that NHE3 exists in physical complexes with dipeptidyl peptidase IV (DPPIV) in brush-border membranes isolated from proximal tubule cells. In contrast to the NHE3-megalin complex (3), which principally resides in the intermicrovillar region of the brush border, a microdomain in which NHE3 is suggested to be inactive (2) or plays a distinct physiological role (10), the NHE3-DPPIV complex distributes mostly in the microvillar microdomain where NHE3 normally functions (11). These findings raised the possibility that association with DPPIV may affect NHE3 surface expression and/or activity.

DPPIV, also known as CD26, is a membrane-associated protein that is widely distributed in numerous tissues, including epithelial and endothelial cells and lymphocytes (42). A soluble form of the peptidase is also present in plasma and other body fluids (23). DPPIV acts by selectively removing NH_2-terminal dipeptides from oligopeptides with a penultimate proline or alanine (19). Through this action, it is able to degrade and inactivate several regulatory peptides including peptide hormones (e.g., glucagon-like peptide-1, glucose-dependent insulinotropic polypeptide, bradykinin), neuropeptides (e.g., substance P, neuropeptide Y), and chemokines (e.g., RANTES, eotaxin) so that its activity is important for many different physiological processes (23, 30).

Inhibitors of DPPIV catalytic activity represent a new class of oral antihyperglycemic agents for the treatment of type 2 diabetes mellitus. The usefulness of these inhibitors rests on their ability of preventing the DPPIV-mediated rapid degradation of glucagon-like peptide-1 which is known to have a number of positive effects on glucose homeostasis including stimulation of glucose-dependent insulin secretion, suppression of glucagon secretion, and slowing of gastric emptying (29). Although used routinely, the renal effects of these inhibitors have not been well-characterized.

It has been previously reported that specific competitive inhibitors that bind to the active site of DPPIV reduce NHE3 activity in cultured opossum kidney proximal tubule (OKP) cells (12). This, in turn, implies that DPPIV enzyme activity plays a tonic role in modulating NHE3 in OKP cells. It is therefore of interest to explore the functional relationship between NHE3 and DPPIV in the native proximal tubule. The purpose of this study was to test the hypothesis that DPPIV, by virtue of its oligomeric association with NHE3, directly or indirectly affects NHE3 activity in the intact proximal tubule in vivo. We demonstrate that administration of the reversible DPPIV inhibitor Lys[$Z(NO_2)$]-pyrrolidide (34, 37, 39, 40) is

Address for reprint requests and other correspondence: A. C. C. Girardi, Heart Institute Laboratory of Genetics and Molecular Cardiology, Univ. of São Paulo School of Medicine, Avenida Dr. Enéas de Carvalho Aguiar, 44, 10° andar, Bloco II, 05403-900, São Paulo, SP, Brazil (e-mail: agirardi@icb.usp.br).

The costs of publication of this article were defrayed in part by the payment of page charges. The article must therefore be hereby marked "*advertisement*" in accordance with 18 U.S.C. Section 1734 solely to indicate this fact.

associated with inhibition of NHE3-mediated $NaHCO_3$ reabsorption in the rat renal proximal tubule. Furthermore, our data demonstrate that there exists an in vivo functional interaction between NHE3 and DPPIV.

MATERIALS AND METHODS

Reagents and antibodies. Reagents were obtained from Sigma (St. Louis, MO) unless otherwise specified. DPPIV inhibitor Lys[Z(NO_2)]-pyrrolidide (I40) and the noninhibitory structurally related compound Lys[Z(NO_2)]-OH were purchased from Bachem (Philadelphia, PA). ^{22}Na and [^{32}P]phosphoric acid were obtained from New England Nuclear Life Science Products (Boston, MA). A monoclonal antibody (mAb) raised to the renal brush-border Na^+-H^+ exchanger (NHE3), clone 2B9 (5), was purchased from Chemicon International (Temecula, CA). A monoclonal antibody to rat DPPIV, clone 5E8, was purchased from Cell Sciences (Canton, MA). A mAb to actin (JLA20) was purchased from Calbiochem (San Diego, CA). Horseradish peroxidase-conjugated goat anti-mouse, goat anti-rabbit, and rabbit anti-goat secondary antibodies were purchased from Zymed Laboratories (San Francisco, CA).

Animal preparation. All animal experiments were approved by the Institute of Biomedical Sciences, University of São Paulo, and conducted in accordance with the guidelines for the care and use of laboratory animals stated by the Brazilian Societies of Experimental Biology. Experiments were performed using male Wistar rats (190–240 g) obtained from the Institute of Biomedical Sciences of the University of São Paulo. Animals had free access to water and standard laboratory chow. Lys[Z(NO_2)]-pyrrolidide and the noninhibitory structurally related compound Lys[Z(NO_2)]-OH were provided in the lyophilized form. For the experiments described, the compounds were dissolved in PBS (10^{-2} M) and adjusted to neutral pH. We administered to experimental rats an injection of 60 $mg \cdot kg^{-1} \cdot day^{-1}$ ip of the DPPIV inhibitor Lys[Z(NO_2)]-pyrrolidide (I40) for 7 days. Rats injected with equal amounts of the noninhibitory compound Lys[Z(NO_2)]-OH served as controls. The concentration of I40 administrated was based on the experiments performed by Steinbrecher et al. (39). For the last 24 h, treated and control rats were maintained in metabolic cages for urine collection. Additionally, some studies were performed in which animals were individually housed in metabolic cages throughout the 7-day treatment. Food and water consumption were determined daily and subsequently normalized by body weight. Arterial blood was collected from the carotid at the time of death for measurements of blood pH, blood bicarbonate concentration, and P_{CO_2}. Plasma was also collected to determine concentrations of sodium, potassium, lithium, and creatinine.

Blood and urine analysis. pH, bicarbonate concentration, and P_{CO_2} were measured on a Radiometer ABL5 blood-gas analyzer (Radiometer, Copenhagen, Denmark). Sodium and potassium concentrations were measured on a 9180 Electrolyte Analyzer (Roche Diagnostics, Mannheim, Germany). Flame photometry (Micronal B262, São Paulo, SP, Brazil) was performed to obtain lithium concentration. Plasma and urine creatinine were measured on a Beckman Coulter Synchron CX7 Analyzer (Beckman Coulter, Fullerton, CA).

Arterial pressure and heart rate determinations. Immediately after administration of the last dose of I40 or its inactive analog, rats underwent anesthesia with ketamine-xylazine-acepromazine (64.9, 3.20, and 0.78 mg/kg ip). The right carotid artery was catheterized with a polyethylene catheter (PE-50, 8 cm, filled with heparinized saline) that was exteriorized in the midscapular region. After recovery, rats were placed in individual cages. Twenty-four hours later, arterial pressure and heart rate were measured in conscious animals. Arterial blood pressure was measured by a pressure transducer (model Deltran DPT-100, Utah Medical Products, Midvale, UT) connected to an amplifier (model AECAD-0804, Solução Integrada, São Paulo, SP, Brazil) and recorded using an interface and software for computer data acquisition (model DI-194RS WinDaq, DataQ Instruments, Akron, OH). Heart rate was determined from the pressure pulse intervals.

Enzyme assays. Both DPPIV (17) and γ-glutamyl transpeptidase (γ-GTP) (41) activities were assayed in kidney homogenates by measuring the release of p-nitroaniline resulting from the hydrolysis of glycylproline p-nitroanilide tosylate and γ-glutamyl p-nitroanilide (Sigma), respectively. DPPIV activity was measured by incubating 10 μl of kidney homogenates with 100 μl of phosphate saline buffer, pH 7.4, containing 2 mM glycylprolyl-p-nitroanilide tosylate for 30 min at 37°C. The mixture was incubated for 30 min at 37°C. The reaction was terminated by the addition of 300 μl 1 M acetate buffer, pH 4.2. For the γ-GTP assay, 10 μl of kidney homogenates were added to the 2-ml reaction mixture containing 4.2 mM L-γ-glutamyl-p-nitroanilide, 52.5 mM glycylglycine, 10.5 mM $MgCl_2$ in 50 mM ammediol buffer, pH 9.3, and incubated for 5 min at 25°C. Determination of p-nitroaniline liberated enzymatically was based on the absorbance at 380 nm. Catalytic activities are expressed as milliunits per milligram of protein, where one unit of enzymatic activity was defined as the amount of enzyme required for the formation of 1 μM p-nitroaniline per minute under the conditions described.

Microvillar membrane vesicle preparation. Immediately after kidney removal, cortices were separated at 4°C and homogenized in K-HEPES buffer (200 mM mannitol, 80 mM HEPES, 41 mM KOH, pH 7.5) containing the protease inhibitors pepstatin A (0.7 μg/ml), leupeptin (0.5 μg/ml), PMSF (40 μg/ml), and K_2EDTA (1 mM). Microvillar membrane vesicles (MMV) were prepared using a method based on Mg^{2+} precipitation and differential centrifugation as previously described (6). Protein concentration was measured by the method of Lowry (27). Rat MMV preparations used in this study were 11- to 14-fold enriched in specific activity of the brush-border membrane marker enzyme γ-GTP relative to kidney homogenates.

Preparation of renal membrane fractions. Renal cortex was dissected cold from recently excised kidneys. Postmitochondrial microsomes were prepared and separated on 15–25% OptiPrep (Nycomed Pharma, Oslo, Norway) gradients essentially as described previously (2, 21). One-milliliter fractions were manually collected from the top and assayed for the presence of villin (H-60, Santa Cruz Biotechnology, Santa Cruz, CA) and megalin (H-245, Santa Cruz Biotechnology) by immunoblotting. *Fraction 1* which was enriched in the microvillar membrane marker villin (low-density gradient fraction) was pelleted by centrifugation and resuspendend in K-HEPES buffer. High-density fractions, which were enriched in megalin, but not villin, were pooled from *fractions 5–6* in the gradient, pelleted, and then resuspended in K-HEPES buffer. The low- and high-density gradient fractions were stored at −80°C. Protein concentration was measured by the method of Lowry et al. (27).

Radioactive sodium uptake. Uptake of ^{22}Na into the membrane vesicles was assayed at room temperature using a rapid filtration technique (28). MMV were washed and equilibrated for 1 h at room temperature in 254 mM mannitol, 35 mM KOH, 68 mM HEPES, 50 mM Mes, pH 6.0. The vesicles were then centrifuged and resuspended in the same medium at a final protein concentration of 10 μg/μl. Uptake experiments were then performed in triplicate by the addition of 10 μl of membrane suspension to 90 μl of experimental solution containing 4×10^5 cpm ^{22}Na, 300 mM mannitol, 42 mM KOH, 80 mM HEPES, pH 7.5. After incubation for 15 s at room temperature, the reaction was terminated by rapid addition of 3.0 ml of an iced "stop solution" consisting of 300 mM mannitol, 42 mM KOH, 80 mM HEPES, pH 7.5. The mixture was immediately poured on a 0.65-μm Millipore filter and washed with an additional 9.0 ml of "stop solution." Filters were then placed in vials containing 3.0 ml Ready Solv HP (Beckman) and counted by scintillation spectroscopy. Values for the nonspecific retention of ^{22}Na by the filters were subtracted from the values for the incubated samples. Some experiments were performed in the presence of 100 μM EIPA to inhibit NHE3 activity.

Sodium-dependent phosphate uptake assays. Uptake of ^{32}P-radiolabeled phosphoric acid was measured at room temperature using a

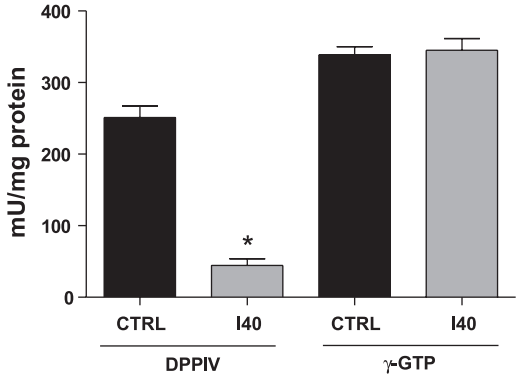

Fig. 1. Reduction of rat renal dipeptidyl peptidase IV (DPPIV) activity by Lys[Z(NO_2)]-pyrrolidide (I40) treatment in vivo. Male Wistar rats were treated with an injection of the reversible DPPIV inhibitor (I40, 60 mg·kg^{-1}·day^{-1} ip) for 7 days. Rats injected with equal amounts of the structurally related noninhibitory compound Lys[Z(NO_2)]-OH served as controls. Activities of DPPIV and γ-glutamyl transpeptidase (γ-GTP) were assayed on whole kidney homogenates as described in MATERIALS AND METHODS. Catalytic activities are expressed as mU/mg protein. Values are means ± SE; n = 24/group. *P < 0.0001 vs. control as determined by ANOVA followed by Tukey's post hoc analysis.

rapid Millipore filtration technique (20). MMV were suspended in a sodium-free medium containing 300 mM mannitol, HEPES·Tris, pH 7.4. Uptake was initiated by mixing 10 μl MMV suspension with 40 μl of transport medium that comprised of 100 mM mannitol, 100 mM NaCl, HEPES·Tris, and ^{32}P-radiolabeled phosphoric acid (2 μCi/ml). To determine non-Na^+ gradient-dependent or diffusive phosphate uptake, 100 mM NaCl was replaced with 100 mM KCl. Uptake was terminated after 10 s by aspiration of the transport medium and washing the cells with ice-cold sodium-free medium. Radioisotopic activity was determined by liquid scintillation spectroscopy. Nonspecific retention of $^{32}PO_4$ was determined and subtracted from the values for the incubated samples.

SDS-PAGE and immunoblotting. Protein samples were solubilized in SDS sample buffer and separated by SDS-PAGE using 7.5% polyacrylamide gels according to Laemmli (22). For immunoblotting, proteins were transferred to polyvinylidene difluoride (PVDF; Immobilon-P; Millipore, Bedford, MA) from polyacrylamide gels at 500 mA for 5 h at 4°C with a Transphor transfer electrophoresis unit (Hoefer Scientific Instruments, San Francisco, CA) and stained with Ponceau S in 0.5% trichloroacetic acid. Entire sheets of PVDF membranes containing transferred proteins were incubated first in Blotto (5% nonfat dry milk and 0.1% Tween 20 in PBS, pH 7.4) for 1–3 h at room temperature to block nonspecific binding of antibody, followed by overnight incubation in primary antibody. The PVDF membrane was subsequently incubated overnight at 4°C with the primary antibody in Blotto at the following concentrations: anti-NHE3 at 1:1,000; anti-DPPIV at 1:500; anti-actin at 1:5,000; anti-villin at 1:1,000; or anti-megalin at 1:200. The membranes were then washed five times in Blotto and incubated for 1 h with the correspondent horseradish peroxidase-conjugated IgG from Zymed (at 1:2,000). Bound antibody was detected with the ECL enhanced chemiluminescence kit (GE Healthcare, Piscataway, NJ), according to the manufacturer's protocols. Multiple exposures of Kodak BioMax MR Film (Kodak, Rochester, NY) were made to ensure that signals were within linear range of the film. The visualized bands were digitized using the ImageScanner (GE HealthCare) and quantified by the ImageQuant program (Molecular Dynamics).

Statistics. All results are reported as means ± SE with n indicating the number of observations. Comparisons between two groups were performed using unpaired t-tests. If more than two groups were compared, statistical significance was determined by ANOVA followed by Tukey's post hoc test. A P value <0.05 was considered significant. The program "Graph Pad Prism 4" (Graph Pad Software, San Diego, CA) was used to calculate significance.

RESULTS

Effect of DPPIV inhibition on NHE3 activity in rat renal proximal tubule. For this study, we administered to experimental rats an injection of 60 mg·kg^{-1}·day^{-1} ip of the highly specific DPPIV inhibitor I40 (34, 37, 39, 40). Rats injected with equal amounts of the noninhibitory compound Lys[Z(NO_2)]-OH served as controls (39). As mentioned earlier, DPPIV is a serine protease that cleaves NH_2-terminal dipeptides from peptides with a penultimate proline or alanine (19). Based on the structural similarity of pyrrolidide to proline, I40 is a dipeptide product analog with high affinity (K_i = 0.271 ± 0.012 μM) for binding to the active site and inhibiting DPPIV (37, 40).

After 7 days of treatment with I40, DPPIV catalytic activity was assayed in kidney homogenates. As seen in Fig. 1, DPPIV enzyme activity in renal homogenates was 257 ± 12 mU/mg protein in control rats, whereas in I40-treated rats it was only 40 ± 7 mU/mg protein (P < 0.0001). In contrast, activity of

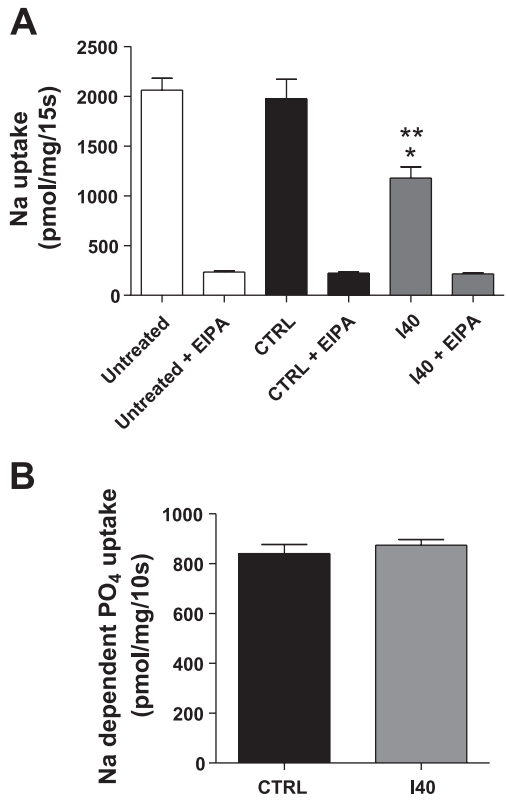

Fig. 2. Effect of DPPIV inhibition on proton-dependent sodium uptake in rat renal microvillar membrane vesicles (MMV). MMV were prepared from untreated (rats administered PBS, n = 4), control (rats administered I40-inactive analog, n = 8), and I40-treated rats (n = 8). A: Na^+-H^+ exchange activity is the proton-dependent uptake of ^{22}Na after 15-s incubation at room temperature. The effect of the DPPIV inhibitor I40 on NHE3 activity was studied in the presence or absence of 100 μM EIPA. Each assay was performed in triplicate. B: sodium-dependent phosphate uptake analysis in rat renal MMV. Uptake of radioactive phosphate was measured by a rapid filtration technique in the presence and absence of external sodium at pH 7.4. Each assay was performed in triplicate. Values are means ± SE. *P < 0.001 vs. untreated and **P < 0.01 vs. control as determined by ANOVA followed by Tukey's post hoc analysis.

another proximal tubule apical membrane enzyme, γ-GTP, did not change in rats treated with the DPPIV inhibitor compared with control rats ($P = 0.75$).

To examine the possible role of DPPIV in modulating NHE3 activity in vivo, Na^+-H^+ exchange activity was assayed in renal MMV prepared from untreated (rats administered PBS, $n = 4$), control (rats administered I40-inactive analog, $n = 8$), and I40-treated rats ($n = 8$). The results of these experiments are shown in Fig. 2*A*. The noninhibitory I40 structurally related compound had no effect on Na^+-H^+ exchange mediated by NHE3 compared with rats that received vehicle (PBS; $P > 0.05$). Conversely, NHE3 activity was significantly reduced in I40-treated rats (962 ± 111 pmol·mg^{-1}·15 s^{-1}) relative to both control (1,827 ± 119 pmol·mg^{-1}·15 s^{-1}) and untreated rats (1,752 ± 194 pmol·mg^{-1}·15 s^{-1}; $P < 0.001$ and $P < 0.01$, respectively). No significant difference among these groups was observed when MMV were assayed in the presence of 100 μM EIPA.

To verify the specificity of the effect of DPPIV inhibition on NHE3 activity, we evaluated whether treatment with I40 would affect the activity of another apical membrane sodium-dependent transporter, the Na-phosphate cotransporter, which had previously found not to be associated with DPPIV (11). Na-phosphate cotransporter activity was measured as ^{32}P-radiolabeled phosphate uptake in the presence of sodium. As indicated in Fig. 2*B*, no detectable difference was observed in the sodium-dependent component of radiolabeled phosphate uptake in the presence of the DPPIV inhibitor I40.

Taken together, these results indicate that DPPIV enzyme activity in renal tissue is markedly reduced by treatment with I40. The inhibition of the catalytic site of DPPIV specifically decreases NHE3 activity by ~45% in rat renal proximal tubule.

Effect of DPPIV inhibitor I40 on NHE3 expression in rat renal proximal tubule. We next examined whether the effect of I40 to reduce NHE3 activity is due to changes in expression and subcellular localization of NHE3.

MMV isolated by divalent cation precipitation were subjected to SDS-PAGE and immunoblotting. As indicated in Fig. 3, DPPIV inhibition led to decreased abundance of MMV-NHE3. Densitometric analyses, corrected to actin expression used as internal control, revealed a decrease of 51 ± 6% on renal microvillar NHE3 protein content, compared with the control group (Fig. 3*B*). Interestingly, not only NHE3 protein expression is downregulated by the inhibition of DPPIV activity but also the expression of DPPIV itself. As seen in the representative immunoblot (Fig. 3*A*), and confirmed by densitometry (Fig. 3*C*), I40 treatment induced a 27 ± 5% decrement on MMV-DPPIV protein levels.

Biemesderfer and colleagues (2) previously showed that NHE3 exists as (at least) two oligomeric forms that are differentially localized to distinct microdomains of the kidney brush border. Approximately 50% of the transporter has a sedimentation coefficient of 9.6S and is enriched in the microvillar membrane. In contrast, the remainder of the NHE3 protein has a sedimentation coefficient of 21S and principally resides in the intermicrovillar cleft region of the kidney brush border (2). Considering these findings, we sought to test the hypothesis that decrement of MMV-NHE3 protein content in response to DPPIV inhibition may possibly be caused by redistribution of NHE3 from the microvillar to the intermicrovillar fraction of kidney brush border. For this purpose, we performed immu-

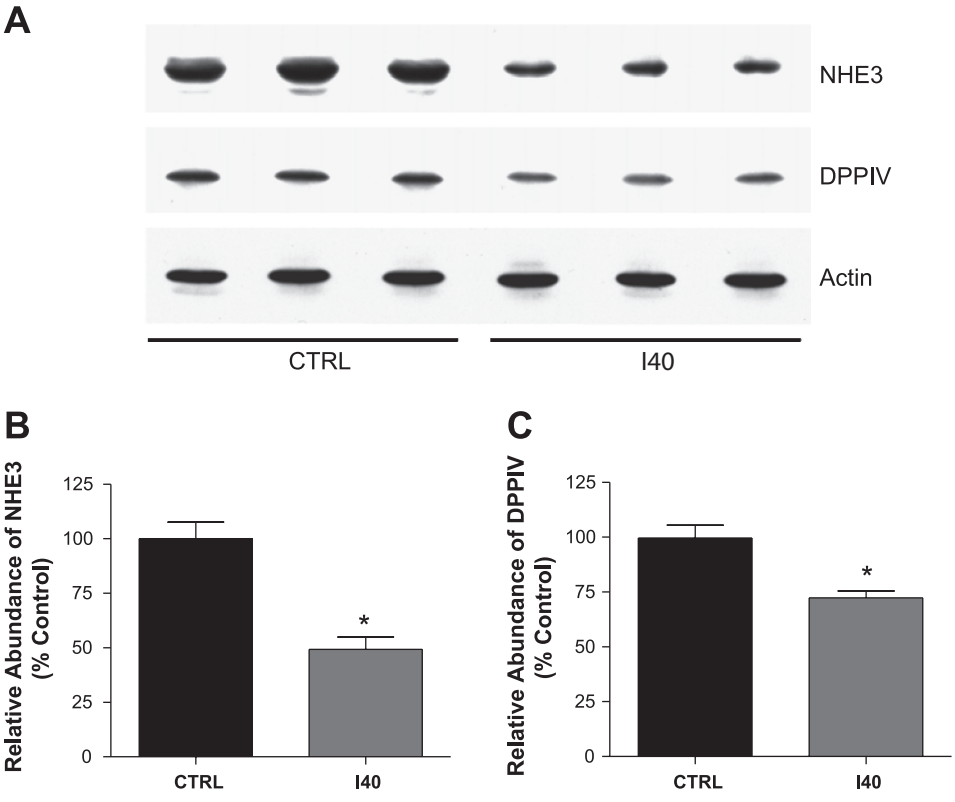

Fig. 3. Effect of DPPIV inhibition on NHE3 and DPPIV protein expression levels in rat renal microvillar membranes. *A*: MMV were prepared by divalent cation aggregation from rats treated with I40 or the noninhibitory compound Lys[Z(NO_2)]-OH (control) for 7 days. Equal amounts of MMV (25 μg protein) were subjected to SDS-PAGE, transferred to a PVDF membrane, and analyzed by immunoblotting. Blots were probed with antibodies to NHE3, DPPIV, and actin (as loading control). Densitometry values for NHE3 (*B*) and DPPIV (*C*) were normalized with actin and plotted as a bar graph. Results are expressed as % of control. Values are means ± SE. *$P = 0.0003$ and **$P = 0.01$ vs. control as determined by unpaired *t*-test.

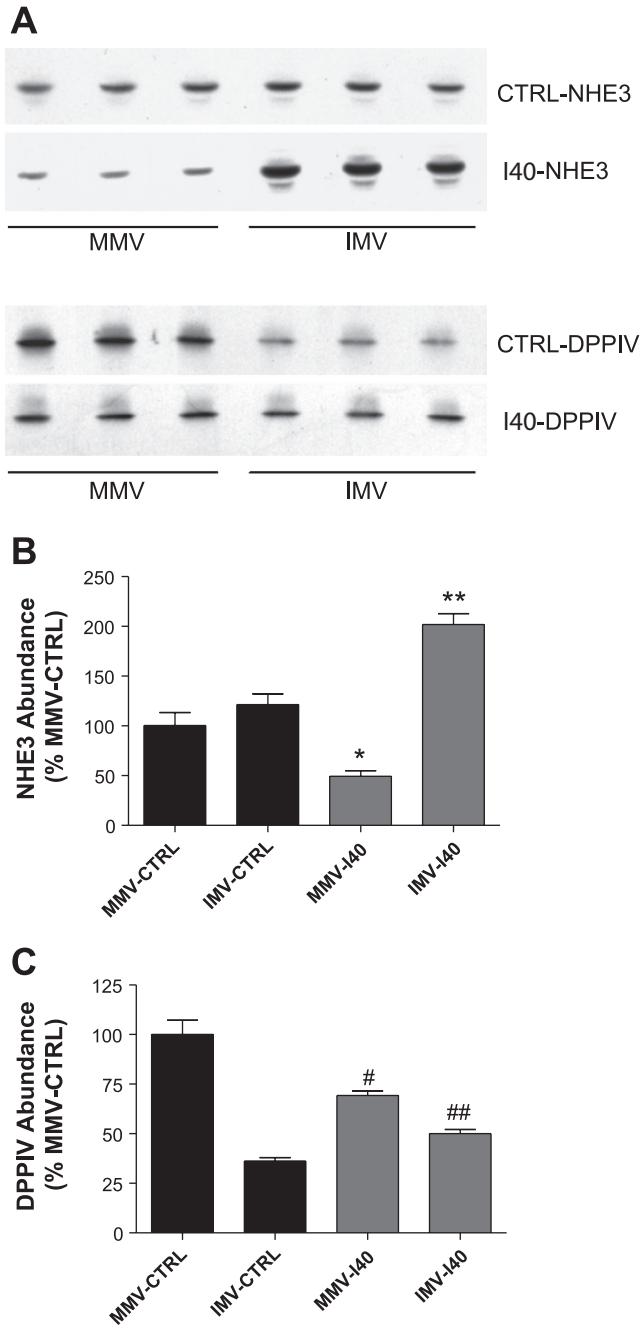

Fig. 4. Changes in subcellular localization of NHE3 and DPPIV in response to a 7-day treatment with the competitive DPPIV inhibitor I40. *A*: rat cortical microsomes from controls (rats administered I40-inactive analog) and I40-treated rats were separated by isopycnic centrifugation using 15–25% OptiPrep density gradients. Equal quantities (25 μg protein) of a light-density fraction enriched in MMV and of a high-density fraction enriched in intermicrovillar markers such as megalin (IMV) were analyzed by immunoblotting. Blots were probed successively with antibodies to NHE3 and DPPIV. Densitometry values for NHE3 (*B*) and DPPIV (*C*) were plotted as a bar graph. Values shown are means ± SE normalized to mean of MMV-CTRL defined as 100%. Values are means ± SE; $n = 4$/group. *$P < 0.05$ vs. MMV-CTRL. **$P < 0.001$ vs. IMV-CTRL. #$P < 0.001$ vs. MMV-CTRL and ##$P < 0.01$ vs. IMV-CTRL. Statistical significance was determined by ANOVA followed by Tukey's post hoc analysis.

noblotting experiments (Fig. 4) using equal quantities (25 μg protein) of a light-density gradient fraction enriched in microvillar membrane proteins (MMV) and a high-density fraction enriched in intermicrovillar membrane proteins (IMV) isolated by density fractionation of total renal cortical membranes. As shown in Fig. 4, *A* and *B*, sustained inhibition of DPPIV activity induced a decrease of 51 ± 7% (MMV-I40 vs. MMV-CTRL, $P < 0.05$) on NHE3 expression in the microvillar-enriched fraction paralleled by an increase of 73 ± 8% (IMV-I40 vs. IMV-CTRL, $P < 0.001$) on the transporter abundance in the intermicrovillar membrane-enriched fraction. A similar pattern of redistribution was observed for DPPIV (Fig. 4, *A* and *C*).

We also analyzed the effect of DPPIV inhibition on total cortical expression of both NHE3 and DPPIV. As illustrated in Fig. 5, nonsignificant differences were found for NHE3 ($P = 0.07$; I40 vs. CTRL) and DPPIV ($P = 0.71$; I40 vs. CTRL) total kidney cortical expression in response to a 7-day treatment with the reversible DPPIV inhibitor I40.

Based on these findings, we conclude that reduction in NHE3 activity is due to its retraction out of the apical-enriched microvillar membrane microdomain of the kidney brush border. The NHE3-associated protein DPPIV redistributes to the intermicrovillar membrane-enriched fraction along with NHE3 indicating a functional interaction between these two proteins in rat renal proximal tubule.

Effect of DPPIV inhibition on renal tubular handling of sodium, fluid, and bicarbonate. Having demonstrated that inhibition of NHE3 in the intact proximal tubule is associated with the decrease in DPPIV catalytic activity, we next verified whether differences with respect to sodium, fluid, and bicarbonate reabsorption could be observed between I40-treated and control rats.

Rats treated with the DPPIV inhibitor I40 for 7 days had significantly increased urine output compared with control rats (I40-treated rats: 39 ± 3 vs. control rats: 65 ± 8 ml/kg body wt; $P < 0.01$) during the collection period of 24 h (Fig. 6*A*). In parallel, the increase in urine output was accompanied by a significant increase in water intake (Table 1). As depicted in Fig. 6*C*, I40-treated rats exhibited a significantly higher fractional sodium excretion compared with control rats (0.88 ± 0.11 vs. 0.54 ± 0.04% in control rats; $P < 0.01$). As seen in Table 1, no increment on food intake was observed between the two groups. In fact, rats administered I40 gain less weight throughout the 7-day period of treatment compared with controls. Whether this effect is due to a transient negative sodium balance is unknown. Of note, some reports showed that long-term treatment with DPPIV inhibitors may cause reduction in body weight gain (33). Nonetheless, to fully address this aspect, a detailed metabolic analysis should be carried out which is beyond the scope of this study.

Blood samples taken after the 7-day treatment period yielded the data presented in Table 2. There were no significant differences between the two groups of animals with respect to any of the blood variables measured. Also, creatinine clearance was unaltered between treated animals and controls (5.5 ± 0.2 vs. 6.0 ± 0.3 $ml \cdot min^{-1} \cdot kg\ body\ wt^{-1}$ in controls; $P = 0.11$) suggesting that glomerular filtration rate was not significantly affected by DPPIV inhibition (Fig. 6*B*).

On the basis that filtered lithium ions are reabsorbed exclusively in proximal tubule, in proportion to the reabsorption of

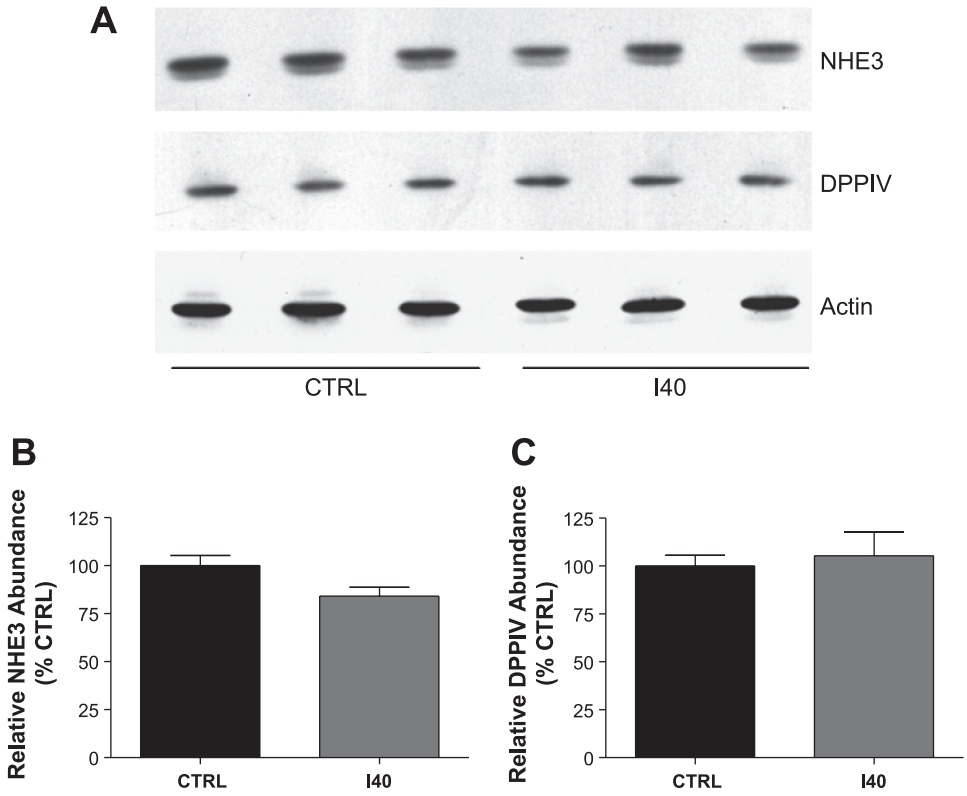

Fig. 5. Effect of DPPIV inhibition on NHE3 and DPPIV protein expression levels in rat renal cortex. *A*: 50 μg of renal cortical membranes isolated from rats treated with I40 or the structurally related noninhibitory compound Lys[Z(NO_2)]-OH (control) were subjected to SDS-PAGE, transferred to a PVDF membrane, and analyzed by immunoblotting. Blots were probed successively with antibodies to NHE3, DPPIV, and actin. Densitometry values for NHE3 (*B*) and DPPIV (*C*) were normalized with actin and plotted as a bar graph. Results are expressed as % of control. Values are means ± SE; $n = 6$/group.

sodium and water, lithium clearance (C_{Li}) is widely used as a measure of end-proximal tubule delivery (43). We found that C_{Li} was significantly higher in rats treated with I40 (3.8 ± 0.5 vs. 2.1 ± 0.1 ml·min^{-1}·kg body wt^{-1} in controls; $P < 0.01$; Fig. 6*D*). Thus impairment in sodium and water reabsorption caused by DPPIV inhibition occurs predominantly, if not exclusively, in the kidney proximal tubule.

Renal sodium homeostasis is one of the major determinants for blood pressure levels. Na^+-H^+ exchange is the major route for apical sodium entry across the proximal tubule, and the NHE3 isoform is responsible for virtually all the Na^+-H^+ exchange activity in this region (1, 4, 5, 26, 38, 44–46). The present results demonstrated that although there was a tendency for reduced systolic (~5%), diastolic (~6%), and mean (~5%) arterial pressures in rats treated with the DPPIV inhibitor I40, this decrease was not statistically significant (Table 2). No significant differences were also observed in heart rate between these two groups of rats (Table 2).

Table 3 summarizes the effect of DPPIV inhibition on plasma and urine acid-base composition. Urine analyses re-

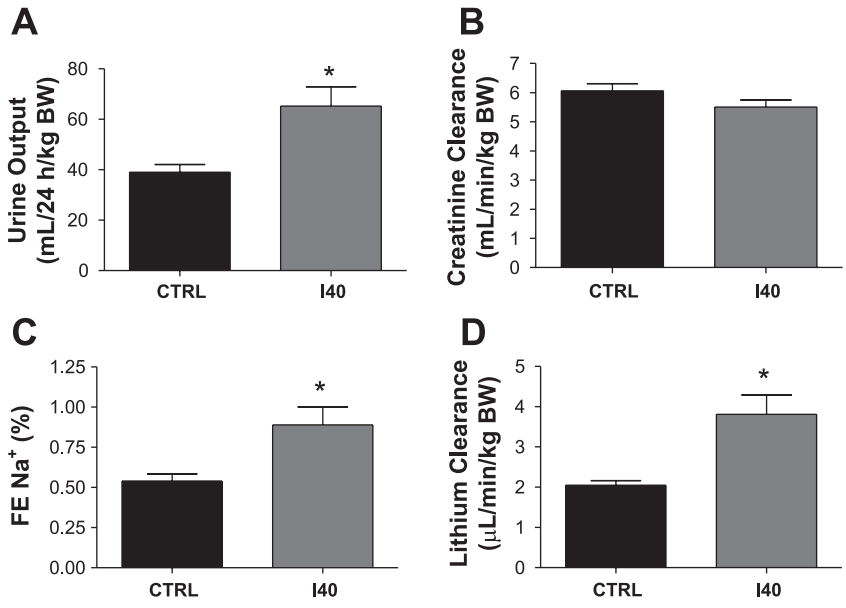

Fig. 6. Effect of DPPIV inhibition on renal function and tubular handling of sodium and fluid. At the end of the protocol period, rats treated with the competitive DPPIV inhibitor I40 ($n = 17$) or its inactive analog (control, $n = 18$) were placed in metabolic cages for collection of 24-h urine samples. *A*: urine output was measured gravimetrically. *B*: creatinine clearance was used to estimate glomerular filtration rate. *C*: fractional sodium excretion was calculated as C_{Na}/C_{Cr} where C_{Na} is Na^+ clearance and C_{Cr} is creatinine clearance. *D*: endogenous lithium clearance (C_{Li}) was calculated as $V \times U_{Li}/P_{Li}$ where V is urine output, U_{Li} is urinary lithium concentration, and P_{Li} is plasma lithium concentration. Renal functional data were corrected by body weight (BW) and expressed per kg BW. Values are means ± SE. *$P < 0.01$ compared with corresponding control values. Statistical significance was assessed by unpaired *t*-test.

Table 1. *Body weight, daily food and water intake in rats treated during 7 days with I40 or the noninhibitory compound Lys[Z(NO$_2$)]-OH (control)*

	Control	I40	*P* Value
Initial body weight, g	218±7	225±8	0.76
Final body weight, g	235±7	235±8	0.41
Body weight gain, %	8.0±1.1	3.7±0.7*	<0.0001
Food intake, g·day^{-1}·kg body wt^{-1}	90±3	92±2	0.67
Water intake, ml·day^{-1}·kg body wt^{-1}	111±5	182±11*	0.0001

Values are means ± SE. Body weight was measured in control and Lys[Z(NO$_2$)]-pyrrolidide (I40)-treated rats (n = 24/group). Measurements of food and water intake were made every day and normalized by body weight (n = 6 rats/group). *Significantly different vs. control, assessed by unpaired t-test.

Table 3. *Plasma electrolytes, creatinine, and acid-base status in rats treated during 7 days with I40 or the noninhibitory compound Lys[Z(NO$_2$)]-OH (control)*

	Control	I40	*P* Value
Plasma Na^+, mM	147.7±2.3	145.3±2.4	0.49
Plasma K^+, mM	4.37±0.09	4.21±0.15	0.37
Plasma creatinine, mg/dl	0.38±0.03	0.44±0.02	0.12
Plasma Li^+, mM	0.19±0.01	0.18±0.01	0.25
Plasma HCO_3^-, mM	23.18±0.30	21.00±0.57	0.07
Plasma pH	7.35±0.01	7.32±0.01	0.07
Plasma P_{CO2}, mmHg	43.14±1.93	39.50±1.09	0.14
Urine pH	6.31±0.10	5.96±0.05*	<0.0001
FE HCO_3^-, %	0.21±0.06	0.18±0.08	0.38

Values are means ± SE; n = 24/group. *Significantly different vs. control, assessed by unpaired t-test.

vealed that rats treated with I40 acidified their urine to a higher extent than controls (5.96 ± 0.05 vs. 6.31 ± 0.11 in control rats, $P < 0.0001$). Fractional bicarbonate excretion was practically equal between the two groups. A trend toward decline of blood pH and bicarbonate concentration was observed in rats treated with I40 for 7 days. However, as seen in Table 3, differences in systemic acid-base status were not statistically significant between control and I40-treated rats.

In concert, changes in renal function triggered by inhibition of DPPIV activity are consistent with downregulation of NHE3-mediated Na^+-H^+ exchange in proximal tubule.

DISCUSSION

NHE3 activity is controlled tightly by several molecular mechanisms, including interaction with binding partner proteins. The biochemical and physiological characterization of these interactions using in vitro and in vivo models will certainly provide new understanding of sodium, bicarbonate, and fluid transport by the kidneys. In the present report, we examined the functional significance of the association of NHE3 with DPPIV in the native rat renal proximal tubule. We found that 7-day treatment with the DPPIV inhibitor Lys [Z(NO$_2$)]-pyrrolidide reduces Na^+-H^+ exchange activity in isolated MMV. Inhibition of microvillar membrane Na^+-H^+ exchange is mainly due to changes in the subcellular localization of NHE3.

The renal brush border is composed of two microdomains that are structurally and functionally distinct (35). The microvillar microdomain consists of villin-rich, actin-based cores that serve to amplify the apical proximal tubule surface area enhancing its capacity to transport substances present in the luminal fluid. At the base of the brush border, the plasma membrane invaginates into the cytoplasm forming the intermicrovillar cleft region. The intermicrovillar microdomain is enriched in megalin and is involved in mediating the initial steps of endocytic internalization in these cells (35). Immunoprecipitation experiments using monoclonal antibodies directed to either DPPIV or megalin have revealed that the pools of NHE3 complexed with DPPIV and megalin are largely distinct. Whereas NHE3-DPPIV complexes predominately reside in the microvilli (11), NHE3-megalin complexes are mainly present in the intermicrovillar clefts (2, 3). Our results indicate that long-term inhibition of DPPIV activity in rats leads NHE3 to shift to the megalin-enriched microdomain. Interestingly, a similar shift in the distribution of DPPIV itself was found in I40-treated rats confirming a functional link between these proteins. These findings are in agreement with a series of studies performed by the laboratory of Dr. A. McDonough in which NHE3 along with DPPIV are coordinately redistributed between the microdomains of the kidney brush border in response to both acute (25, 49) and chronic stimuli (48, 50).

Table 2. *Arterial blood pressure and heart rate in rats treated during 7 days with I40 or the noninhibitory compound Lys[Z(NO$_2$)]-OH (control)*

	Control	I40	*P* Value
Systolic arterial pressure, mmHg	123±3	117±3	0.22
Diastolic arterial pressure, mmHg	97±5	91±4	0.49
Mean arterial pressure, mmHg	111±4	105±3	0.37
Heart rate, beats/min	346±16	321±14	0.26

Values are means ± SE. Systolic arterial pressure, diastolic arterial pressure, mean arterial pressure, and heart rate were measured in conscious animals 24 h after administration of the last dose of I40 (n = 7) or its inactive analog (n = 6) as described in MATERIALS AND METHODS.

The precise physiological role of NHE3 in the intermicrovillar domain is difficult to ascertain. Studies by Biemesderfer and colleagues (3) suggest that NHE3 may be inactive when it is complexed with megalin. On the other hand, Yang et al. (47) showed that NHE3 is active in high-density gradient fractions that are enriched in megalin but not villin. It has also been demonstrated in vitro using OK cells that NHE3 plays a role in the initial endosomal acidification necessary for receptor-mediated albumin internalization (10). Anyhow, it appears to be consensual that the pool of NHE3 located in the intermicrovillar region of the brush border is not primarily involved with sodium reabsorption. Therefore, shifts in NHE3 redistribution have important consequences for the regulation of salt and water reabsorption by the renal proximal tubule.

Currently, several DPPIV inhibitors are undergoing clinical trials to evaluate the usefulness of these agents for the treatment of type 2 diabetes mellitus (DM2). The therapeutic utility of the DPPIV inhibitors rests mainly on their ability to prolong the half-life of insulin-releasing hormones (incretins), including glucagon-like peptide 1 (GLP-1) and the glucose-dependent insulinotropic hormone (GIP) (29). Every year an increasing number of studies are published evaluating the clinical efficacy and tolerability of these inhibitors in patients with

DM2. To the authors' knowledge, this is the first report describing the renal effects of DPPIV inhibition. We found that rats treated with the DPPIV inhibitor I40 for 7 days present an increase in fractional sodium excretion (65%). Sodium influx provides the principal driving force for reabsorption of water in the proximal tubule cell, and a reduction in sodium reabsorption is coupled with a reduction in water reabsorption. Accordingly, DPPIV inhibition increases urine output by ~70%.

Despite the fact that increases in urine output and fractional sodium excretion were associated with DPPIV inhibition, no statistically significant differences with respect to blood pressure were observed in I40-treated animals. This may be explained by the existence of compensatory mechanisms such as upregulation of the renin-angiotensin-aldosterone system, as observed in mice lacking the NHE3 Na^+-H^+ exchanger, that limit gross perturbations in overall volume homeostasis (38).

With regard to systemic acid-base status, I40-treated rats had slight decreases in blood pH and bicarbonate concentration. However, under our experimental conditions, these changes did not reach statistical significance. These observations are consistent with a partial inhibition of NHE3-mediated proton secretion. Since DPPIV does not seem to affect later nephron segments, reduction of NHE3 activity in proximal tubule may be fully compensated by increased urinary acid excretion and bicarbonate regeneration at downstream segments preventing the occurrence of acid-base disorders. Accordingly, urinary pH fell significantly in the I40-treated group.

The affector mechanisms by which DPPIV inhibition reduces NHE3 function are yet to be established. DPPIV is known to degrade a variety of peptide hormones, cytokines, and chemokines (23, 30). Accordingly, there is a high likelihood that DPPIV catalytic activity exerts a tonic role in stimulating NHE3 by processing an inhibitory peptide involved in regulation of the transporter. The effect of DPPIV inhibition on NHE3 activity might thereby be mediated by increasing the half-life of this candidate peptide. One such candidate is the DPPIV substrate GLP-1. GLP-1 is a gastrointestinal hormone secreted into the circulation in response to ingested nutrients. GLP-1 produces multiple physiological effects including enhancement of glucose-mediated insulin secretion, inhibition of glucagon release, promotion of satiety, and inhibition of gastric emptying (9, 18). Renal effects of GLP-1 have been documented by several recent studies undertaken in primary porcine proximal tubular cells (36), rats (24, 31), and humans (15, 16). Intravenous infusion of pharmacological doses of GLP-1 induces a diuretic and natriuretic response by decreasing sodium reabsorption in the proximal tubule (15, 16, 31). Interestingly, in healthy and insulin-resistant obese subjects GLP-1 infusion not only increases sodium excretion but also reduces proton secretion, implicating a direct effect of GLP-1 on Na^+-H^+ exchange (15).

Each protein typically has a large number of alternative interaction partners and the selectivity of these interactions determines its responses to extracellular stimuli. It is of interest to mention that on the surface of the highly invasive 1-LN human prostate tumor cell line, plasminogen type II (Pg 2) forms a multimeric complex with both NHE3 and DPPIV. Pg 2 binding to DPPIV in this cell type induces an intracellular calcium signaling cascade that is accompanied by a rise in intracellular pH. The authors postulated that the interaction of Pg 2 with DPPIV and NHE3 has the potential to regulate simultaneously calcium signaling and Na^+-H^+ exchange necessary to tumor cell invasiveness (14). Preliminary studies from overlay experiments demonstrate that NHE3 and DPPIV do not bind directly to each other in renal brush-border membranes, indicating that additional accessory proteins are required for this association to occur (13). Further biochemical and functional studies should allow us to determine which interaction partners are relevant for mediating the modulatory effect of DPPIV on NHE3 in proximal tubule cells and to define their relative contributions under physiological and pathological conditions.

In summary, these findings indicate that inhibition of DPPIV catalytic activity is associated with inhibition of NHE3-mediated $NaHCO_3$ reabsorption in the native renal proximal tubule. Inhibition of apical Na^+-H^+ exchange results from changes in subcellular localization of NHE3. Moreover, these studies underscore the functional importance of the association between NHE3 and DPPIV in rat renal proximal tubule.

GRANTS

This work was supported by Fundação de Amparo à Pesquisa do Estado de São Paulo (FAPESP) Grants 05/52102-5 and 07/52945-8 to A. C. C. Girardi, 04/01683-5 to G. Malnic and N. A. Rebouças, and 02/13684-0 to L. V. Rossoni; and by Conselho Nacional de Desenvolvimento Científico e Tecnológico. L. E. Fukuda was supported by a Scientific Initiation Fellowship award from FAPESP.

Present address of A. C. C. Girardi: Laboratory of Genetics and Molecular Cardiology, Heart Institute, University of São Paulo School of Medicine, 05403-900, São Paulo, SP, Brazil.

REFERENCES

1. **Amemiya M, Loffing J, Lotscher M, Kaissling B, Alpern RJ, Moe OW.** Expression of NHE-3 in the apical membrane of rat renal proximal tubule and thick ascending limb. *Kidney Int* 48: 1206–1215, 1995.
2. **Biemesderfer D, DeGray B, Aronson PS.** Active (9.6 s) and inactive (21 s) oligomers of NHE3 in microdomains of the renal brush border. *J Biol Chem* 276: 10161–10167, 2001.
3. **Biemesderfer D, Nagy T, DeGray B, Aronson PS.** Specific association of megalin and the Na^+/H^+ exchanger isoform NHE3 in the proximal tubule. *J Biol Chem* 274: 17518–17524, 1999.
4. **Biemesderfer D, Pizzonia J, Abu-Alfa A, Exner M, Reilly R, Igarashi P, Aronson PS.** NHE3: a Na^+/H^+ exchanger isoform of renal brush border. *Am J Physiol Renal Fluid Electrolyte Physiol* 265: F736–F742, 1993.
5. **Biemesderfer D, Rutherford PA, Nagy T, Pizzonia JH, Abu-Alfa AK, Aronson PS.** Monoclonal antibodies for high-resolution localization of NHE3 in adult and neonatal rat kidney. *Am J Physiol Renal Physiol* 273: F289–F299, 1997.
6. **Booth AG, Kenny AJ.** A rapid method for the preparation of microvilli from rabbit kidney. *Biochem J* 142: 575–581, 1974.
7. **Burckhardt G, Di Sole F, Helmle-Kolb C.** The Na^+/H^+ exchanger gene family. *J Nephrol* 5: S3–S21, 2002.
8. **Donowitz M, Li X.** Regulatory binding partners and complexes of NHE3. *Physiol Rev* 87: 825–872, 2007.
9. **Drucker DJ.** Glucagon-like peptides. *Diabetes* 2: 159–169, 1998.
10. **Gekle M, Drumm K, Mildenberger S, Freudinger R, Gabner B, Silbernagl S.** Inhibition of Na^+-H^+ exchange impairs receptor-mediated albumin endocytosis in renal proximal tubule-derived epithelial cells from opossum. *J Physiol* 520: 709–721, 1999.
11. **Girardi AC, Degray BC, Nagy T, Biemesderfer D, Aronson PS.** Association of Na^+-H^+ exchanger isoform NHE3 and dipeptidyl peptidase IV in the renal proximal tubule. *J Biol Chem* 276: 46671–46677, 2001.
12. **Girardi AC, Knauf F, Demuth H, Aronson PS.** Role of dipeptidyl peptidase IV in regulating activity of Na^+-H^+ exchanger isoform NHE3 in proximal tubule cells. *Am J Physiol Cell Physiol* 287: C1238–C1245, 2004.

13. **Girardi AC, Thomson RB, Aronson PS.** Identification of domain of Na/H exchanger NHE3 mediating association with dipeptidyl peptidase IV (DPPIV) (Abstract). *FASEB J* 19: 140A:116.11, 2005.
14. **Gonzalez-Gronow M, Misra UK, Gawdi G, Pizzo SV.** Association of plasminogen with dipeptidyl peptidase IV and Na^+/H^+ exchanger isoform NHE3 regulates invasion of human 1-LN prostate tumor cells. *J Biol Chem* 280: 27173–27178, 2005.
15. **Gutzwiller JP, Hruz P, Huber AR, Hamel C, Zehnder C, Drewe J, Gutmann H, Stanga Z, Vogel D, Beglinger C.** Glucagon-like peptide-1 is involved in sodium and water homeostasis in humans. *Digestion* 73: 142–150, 2006.
16. **Gutzwiller JP, Tschopp S, Bock A, Zehnder CE, Huber AR, Kreyenbuehl M, Gutmann H, Drewe J, Henzen C, Goeke B, Beglinger C.** Glucagon-like peptide 1 induces natriuresis in healthy subjects and in insulin-resistant obese men. *J Clin Endocrinol Metab* 89: 3055–3061, 2004.
17. **Hino M, Fuyamada H, Hayakawa T, Nagatsu T, Oya H.** X-Prolyl dipeptidyl-aminopeptidase activity, with X-proline p-nitroanilides as substrates, in normal and pathological human sera. *Clin Chem* 22: 1256–1261, 1976.
18. **Holst JJ.** Glucagon-like peptide-1, a gastrointestinal hormone with a pharmaceutical potential. *Curr Med Chem* 11: 1005–1017, 1999.
19. **Kenny AJ, Booth AG, George SG, Ingram J, Kershaw D, Wood EJ, Young AR.** Dipeptidyl peptidase IV, a kidney brush-border serine peptidase. *Biochem J* 157: 169–182, 1976.
20. **Kiebzak GM, Sacktor B.** Effect of age on renal conservation of phosphate in the rat. *Am J Physiol Renal Fluid Electrolyte Physiol* 251: F399–F407, 1986.
21. **Kocinsky HS, Girardi AC, Biemesderfer D, Nguyen T, Mentone S, Orlowski J, Aronson PS.** Use of phospho-specific antibodies to determine the phosphorylation of endogenous Na^+/H^+ exchanger NHE3 at PKA consensus sites. *Am J Physiol Renal Physiol* 289: F249–F258, 2005.
22. **Laemmli UK.** Cleavage of structural proteins during the assembly of the head of bacteriophage T4. *Nature* 227: 680–685, 1970.
23. **Lambeir AM, Durinx C, Scharpe S, De Meester I.** Dipeptidyl-peptidase IV from bench to bedside: an update on structural properties, functions, and clinical aspects of the enzyme DPP IV. *Crit Rev Clin Lab Sci* 40: 209–294, 2003.
24. **Larsen PJ, Fledelius C, Knudsen LB, Tang-Christensen M.** Systemic administration of the long-acting GLP-1 derivative NN2211 induces lasting and reversible weight loss in both normal and obese rats. *Diabetes* 50: 2530–2539, 2001.
25. **Leong PK, Devillez A, Sandberg MB, Yang LE, Yip DK, Klein JB, McDonough AA.** Effects of ACE inhibition on proximal tubule sodium transport. *Am J Physiol Renal Physiol* 290: F854–F863, 2006.
26. **Lorenz JN, Schultheis PJ, Traynor T, Shull GE, Schnermann J.** Micropuncture analysis of single-nephron function in NHE3-deficient mice. *Am J Physiol Renal Physiol* 277: F447–F453, 1999.
27. **Lowry OH, Rosebrough NJ, Farr AL, Randall RG.** Protein measurement with the Folin phenol reagent. *J Biol Chem* 193: 265–275, 1951.
28. **Mahnensmith RL, Aronson PS.** Interrelationships among quinidine, amiloride, and lithium as inhibitors of the renal Na^+-H^+ exchanger. *J Biol Chem* 260: 12586–12592, 1985.
29. **McIntosh CH, Demuth HU, Pospisilik JA, Pederson R.** Dipeptidyl peptidase IV inhibitors: how do they work as new antidiabetic agents? *Regul Pept* 128: 159–165, 2004.
30. **Mentlein R.** Dipeptidyl-peptidase IV (CD26)–role in the inactivation of regulatory peptides. *Regul Pept* 85: 9–24, 1999.
31. **Moreno C, Mistry M, Roman RJ.** Renal effects of glucagon-like peptide in rats. *Eur J Pharmacol* 434: 163–167, 2002.
32. **Orlowski J, Grinstein S.** Diversity of the mammalian sodium/proton exchanger SLC9 gene family. *Pflügers Arch* 447: 549–565, 2004.
33. **Reimer MK, Holst JJ, Ahren B.** Long-term inhibition of dipeptidyl peptidase IV improves glucose tolerance and preserves islet function in mice. *Eur J Endocrinol* 146: 717–727, 2002.
34. **Reinhold D, Bank U, Buhling F, Lendeckel U, Faust J, Neubert K, Ansorge S.** Inhibitors of dipeptidyl peptidase IV induce secretion of transforming growth factor-β_1 in PWM-stimulated PBMC and T cells. *Immunology* 91: 354–360, 1997.
35. **Rodman JS, Seidman L, Farquhar MG.** The membrane composition of coated pits, microvilli, endosomes, and lysosomes is distinctive in the rat kidney proximal tubule cell. *J Cell Biol* 102: 77–87, 1986.
36. **Schlatter P, Beglinger C, Drewe J, Gutmann H.** Glucagon-like peptide 1 receptor expression in primary porcine proximal tubular cells. *Regul Pept* 141: 120–128, 2007.
37. **Schön E, Born I, Demuth HU, Faust J, Neubert K, Steinmetzer T, Barth A, Ansorge S.** Dipeptidyl peptidase IV in the immune system. Effects of specific enzyme inhibitors on activity of dipeptidyl peptidase IV and proliferation of human lymphocytes. *Biol Chem Hoppe Seyler* 372: 305–311, 1991.
38. **Schultheis PJ, Clarke LL, Meneton P, Miller ML, Soleimani M, Gawenis LR, Riddle TM, Duffy JJ, Doetschman T, Wang T, Giebisch G, Aronson PS, Lorenz JN, Shull GE.** Renal and intestinal absorptive defects in mice lacking the NHE3 Na^+/H^+ exchanger. *Nat Genet* 19: 282–285, 1998.
39. **Steinbrecher A, Reinhold D, Quingley L, Gado A, Tresser N, Izkison L, Born I, Faust J, Neubert K, Martin R, Ansorge S, Brocke S.** Targeting dipeptidyl peptidase IV (CD26) supresses autoimmune encephalomyelitis and upregulates TGF-β_1 secretion in vivo. *J Immunol* 166: 2041–2048, 2001.
40. **Stockel-Maschek A, Stiebitz B, Born I, Faust J, Werner M, Neubert K.** Potent inhibitors of dipeptidyl peptidase IV and their mechanisms of inhibition. *Adv Exp Med Biol* 477: 117–123, 2000.
41. **Szasz G.** A kinetic photometric method for serum γ-glutamyl transpeptidase. *Clin Chem* 15: 124–136, 1969.
42. **Tanaka T, Camerini D, Seed B, Torimoto Y, Dang NH, Kameoka J, Dahlberg HN, Schlossman SF, Morimoto C.** Cloning and functional expression of the T cell activation antigen CD26. *J Immunol* 149: 481–486, 1992.
43. **Thomsen K.** Lithium clearance: a new method for determining proximal and distal reabsorption of sodium and water. *Nephron* 37: 217–223, 1984.
44. **Vallon V, Schwark JR, Richter K, Hropot M.** Role of Na^+/H^+ exchanger NHE3 in nephron function: micropuncture studies with S3226, an inhibitor of NHE3. *Am J Physiol Renal Physiol* 278: F375–F379, 2000.
45. **Wang T, Hropot M, Aronson PS, Giebisch G.** Role of NHE isoforms in mediating bicarbonate reabsorption along the nephron. *Am J Physiol Renal Physiol* 281: F1117–F1122, 2001.
46. **Wang T, Yang CL, Abbiati T, Schultheis PJ, Shull GE, Giebisch G, Aronson PS.** Mechanism of proximal tubule bicarbonate absorption in NHE3 null mice. *Am J Physiol Renal Physiol* 277: F298–F302, 1999.
47. **Yang LE, Leong PK, Chen JO, Patel N, Hamm-Alvarez SF, McDonough AA.** Acute hypertension provokes internalization of proximal tubule NHE3 without inhibition of transport activity. *Am J Physiol Renal Physiol* 282: F730–F740, 2002.
48. **Yang LE, Leong PK, McDonough AA.** Reducing blood pressure in SHR with enalapril provokes redistribution of NHE3, NaPi2 and NCC and decreases NaPi2 and ACE abundance. *Am J Physiol Renal Physiol* 293: F1197–F1208, 2007.
49. **Yang LE, Leong PK, Shaohua YE, Campese VM, McDonough AA.** Responses of proximal tubule sodium transporters to acute injury-induced hypertension. *Am J Physiol Renal Physiol* 284: F313–F322, 2003.
50. **Yang LE, Zhong H, Leong PK, Perianayagam A, Campese VM, McDonough AA.** Chronic renal injury-induced hypertension alters renal NHE3 distribution and abundance. *Am J Physiol Renal Physiol* 284: F1056–F1065, 2003.